Fracture 1977, Volume 3, ICF4, Waterloo, Canada, June 19 - 24, 1977

SELF-SIMILAR PRESSURE PROFILES IN THE SYMMETRICALLY EXTENDING PLANE CRACK

Finn Ouchterlony*

INTRODUCTION

Much of the author's recent work has involved Fracture Mechanics analysis of rock destruction. In one case, the different stages of the breaking process in rock blasting were modelled by various static radial crack systems in [1]. Another case, which prompted the work in [2], is the splitting of plane rectangular slabs of rock or concrete by wedging tools. A static analysis of mechanically induced rock fractures may be adequate but in rock blasting it is sure to leave out vital parts such as stress wave effects, crack branching phenomena, and the crack propagation speed. This note concerns the latter part. It is based on the author's report [3] and illustrates the effects of gas penetration on the energy release rates at the tips of a symmetrically extending plane crack.

Since the advent of Broberg's analysis [4] many papers on self-similarly extending cracks in elastic media have appeared, see for example [5 - 12] for in-plane situations. The papers by Willis [7] and Norwood [9 - 10] outline general solution procedures but we prefer to base our analysis on the papers by Craggs [5] and Cherepanov and Afanas'ev [8]. It is restricted to symmetric crack extension even though Norwood [10] and Brock [11 - 12] recently have treated some non-symmetric cases and it leads to a Green's function for the stress intensity factor which is analogous to the static one derived by Sih et al [13]. A numerical integration gives results for any symmetric self-similar pressure profile.

PROBLEM FORMULATION AND SOLUTION

Consider the following conditions in plane linear elastodynamics: At $t = 0$ a crack is somehow initiated at the origin of a polar coordinate system (r, θ) in an undisturbed homogeneous medium described by the Young's modulus E and the Poisson'a ratio ν. It's tips propagate in opposite directions along the x-axis with the same constant velocity v which is less than the Rayleigh wave velocity c_R and thus they lie inside the shear wave front at $r = c_2t$, see Figure 1. The crack faces are opened by two pairs of concentrated line loads of magnitude $F = pvt$ which are moving in opposite directions with the velocity $v_F < v$. The disturbed medium is encompassed by the longitudinal wavefront at $r = c_1t$. The boundary conditions along the x-axis are

$$\left.\begin{aligned} & v_\theta = 0 \text{ when } |x| > vt \text{ and} \\ & \sigma_\theta = pvt[\delta(x+v_Ft) + \delta(x-v_Ft)]H(t) \text{ when } |x| < vt \;. \end{aligned}\right\} \qquad (1)$$

* Swedish Detonic Research Foundation, P. O. Box 32058, S-12611 Stockholm, Sweden

Here $\delta(t)$ denotes the delta function and $H(t)$ the unit step function.

The problem consists of solving the governing wave equations with the appropriate initial and boundary conditions. The method of solution follows in the vein of Craggs [14, 5] and Cherepanov and Afanas'ev [8]. The self-similarity of the problem reduces the independent variables to r/t and θ. The semi-circular regions above the x-axis and inside the respective wave fronts c_1t and c_2t are mapped on the upper halves of the ζ_1 and ζ_2 planes respectively with

$$\zeta_j = \frac{1}{r}\,[c_j t \cos\theta + i\sqrt{(c_j t)^2 - r^2}\,\sin\theta] \text{ and } j = 1,\, 2\,. \tag{2}$$

The whole problem then reduces to a Keldysh-Sedov problem for one analytic function in the half-plane $\mathrm{Im}\zeta_1 > 0$.

The details of the solution are found in [3]. For both tips, the resulting expression for the stress intensity factor becomes

$$K_I(v,t,s) = \frac{2pvt}{\sqrt{\pi vt}} \cdot \frac{f(sv)}{f(v)} \cdot \frac{F(v,s)}{\sqrt{1-s^2}}\,. \tag{3}$$

Here $s = v_F/v$ denotes the relative speed of the loading points, $f(v)$ denotes a universal function of the crack speed given by

$$f(v) = \sqrt{1-M_1^2}/(1-\nu)R(v) \text{ where} \tag{4}$$

$$R(v) = -[(2-M_2^2)^2 - 4\sqrt{(1-M_1^2)(1-M_2^2)}]/M_2^2 \tag{5}$$

denotes the Rayleigh function with $M_1 = v/c_1$, and $M_2 = v/c_2$ being Mach numbers and m the ratio c_1/c_2, and $F(v,s)$ denotes the expression

$$F(v,s) = \left\{-\left[\frac{4P(v,s)}{m^2R(sv)} + \frac{s^2}{1-s^2}\right] \cdot [M(v) - L(v) + 4J(v,s)] + \right.$$
$$\left. + 8\,N(v,s)\right\}(1-s^2)/L(v)\,. \tag{6}$$

The function $F(v,s)$ contains in turn the following functional expressions: First there is $P(v,s)$ given by

$$P(v,s) = \frac{(2-s^2M_2^2)\;(6-8s^2M_1^2+s^2M_2^2)}{4(1-s^2M_1^2)} - (3-2s^2M_2^2)\sqrt{\frac{1-s^2M_1^2}{1-s^2M_2^2}}\,. \tag{7}$$

Then we have the well known Broberg function [4]

$$L(v) = \left[\frac{(M_2^2-2M_1^2)^2}{1-M_1^2} + 4M_1^2\right]K_1 - \left[\frac{(2-M_2^2)^2}{1-M_1^2} + 4\right]E_1 - 4M_2^2K_2 + 8E_2\,, \tag{8}$$

where K_1 and E_1 denote complete elliptic integrals of the first and second kind respectively with the modulus $\sqrt{1-M_1^2}$ and the definition of index 2 follows in analogy. For details see Byrd and Friedmann [15]. Next,

$$M(v) = M_1^2\left[\frac{4}{3} + \frac{(2-M_2^2)^2}{1-M_1^2}\right]K_1 - \left[\frac{8}{3}\,(1+M_1^2)+4(1-M_2^2) + \frac{(2-M_2^2)^2}{1-M_1^2}\right]E_1$$
$$- \frac{16}{3}M_2^2K_2 + \frac{4}{3}\,(8-M_2^2)E_2\,. \tag{9}$$

The functions $J(v,s)$ and $N(v,s)$, finally, both contain complete elliptic integrals of the third kind. π_1 has the same modulus as K_1 and E_1 and the parameter $n_1^2 = (1-M_1^2)/(1-s^2M_1^2)$. π_2 is found by switching the indici. The expressions read

$$J(v,s) = -\left[\frac{(2-s^2M_2^2)^2}{4(1-s^2M_1^2)}M_1^2\pi_1 - E_1\right]/s^2 + \left[(2+2M_1^2-3M_2^2)E_1 - M_1^2K_1\right]/3$$
$$+ (M_2^2\pi_2 - E_2)/s^2 - \left[(2-M_2^2)E_2 - M_2^2K_2\right]/3 \text{ and} \tag{10}$$

$$s^2N(v,s) = \frac{(2-s^2M_2^2)(2+s^2M_2^2-4s^2M_1^2)}{4(1-s^2M_1^2)}M_1^2\pi_1 - E_1 - (M_2^2\pi_2 - E_2)$$
$$+ \frac{(2-s^2M_2^2)^2}{(1-s^2M_1^2)}\left[(1-s^2M_1^2-n_1^2)\pi_1 - E_1 + s^2M_1^2K_1\right]/8(1-s^2)$$
$$- \left[(1-s^2M_2^2-n_2^2)\pi_2 - E_2 + s^2M_2^2K_2\right]/2(1-s^2)\,. \tag{11}$$

In the quasi-static limit equation (3) yields the same result as would Sih et al [13] for a symmetric loading.

The case when the forces act at the origin is contained in equation (3). Setting $v_F = s = 0$ we obtain

$$K_I(v,t,0) = \frac{2F}{\sqrt{\pi vt}} \cdot [M(v)/L(v) - 1]/f(v)\,. \tag{12}$$

Somewhat surprisingly, this implies that the stress intensity factor, and hence the energy release rate, will become zero at a crack speed v_{max} which is less than the Rayleigh wave speed. See Figure 2 for details.

ENERGY RELEASE RATES CAUSED BY SELF-SIMILAR PRESSURE PROFILES

Our purpose is to study the effects of gas penetration on the energy release rate at various crack speeds. More specifically, we choose a one parameter family of binomial type pressure profiles given by

$$p(s,q) = p_o(1+q)(1-|s|)^q \quad \text{when} \quad -1 \leq s \leq 1\,. \tag{13}$$

Here p_o is some reference pressure and the parameter q is a measure of the peakedness or, equivalently, the gas penetration. All pressure profiles exert the same opening force on the crack faces due to the factor $(1+q)$. The stress intensity factor is obtained from an integration of equation (3) with p(s,q) as a weight functions as

$$K_I(v,t,q) = \int_0^1 K_I(v,t,s)\ p(s,q)ds \ . \qquad (14)$$

The energy release rate in turn is given by the universal relation

$$G_I(v,t,q) = (1-\nu^2)K_I^{\,2}(v,t,q)f(v)/E \ , \qquad (15)$$

see Freund and Clifton [16] for example. Plane strain conditions are assumed.

We prefer to present normalized values g of the energy release rates with the static Broberg crack taken as the reference state. Thus

$$g(v,q) = G_I(v,t,q)/G_{Io} \quad \text{where } G_{Io} = \pi(1-\nu^2)p_0^{\,2}a/E \ , \qquad (16)$$

and a = vt is the instantaneous crack length. Hereby g(v,q) becomes independent of a. With the aid of equations (3), and (13 - 16), we may write

$$g(v,q) = g(v,0) \cdot \left[\frac{2(1-\nu)(1+q)L(v)}{\pi m} \int_0^1 (1-s)^q f(sv)\ \frac{F(v,s)}{\sqrt{1-s^2}}\ ds\right]^2 , \qquad (17)$$

where g(v,0) is the normalized energy release rate of the Broberg crack which is given by

$$g(v,0) = m^2M_1^{\,4}/L^2(v)f(v) \ . \qquad (18)$$

The squared factor in equation (17) is denoted I(v,q) and must be evaluated numerically. For the Broberg crack a weighted Gauss-Chebyshev formula with ten sampling points yields $I^2(v,0) = 1.000$ and that confirms equation (3).

It is also possible to deduce other limiting forms for g(v,q). From equation (12) there follows that for an infinitely peaked pressure distribution the normalized energy release rate is given by

$$\lim_{q\to\infty} g(v,q) = \frac{4}{\pi^2}\ [M(v)/L(v)-1]^2/f(v) \ . \qquad (19)$$

For a static crack the results of Sih et al [13] yield the formula

$$g(0,q) = \frac{4}{\pi^2}\left[(q+1) \sum_{k=0}^{\infty} (-1)^k (1/2)_k/(q+1/2)_{k+1}\right]^2 , \qquad (20)$$

where the expression $(\ )_k$ denotes the Pochhammer's symbol.

The results of the calculations are plotted in Figure 3 where g(v,q) is shown as a function of crack speed for ν = 1/3 and with q as a parameter.

The exact limiting forms for q = 0 and q = ∞, given by equations (18) and (19) respectively, are represented by full lines. For intermediate values of q, where a numerical evaluation of I(v,q) is necessary, the results are indicated by broken lines. The static limit given by equation (20) is drawn as circles on the vertical axis and the limiting speed on the horizontal one.

We observe that the extent of gas penetration has a profound effect on the energy release rate. At one extreme, total gas penetration is modelled by q = 0 and the curve g(v,0) may be regarded as an upper limit to possible values of the energy release rate. Even a slight decrease in the gas penetration will lower it markedly. For a linearly decreasing gas pressure for example, when q = 1, the available energy is reduced to about half or less. For a more realistic pressure profile we would expect it to drop even more and to approximately correspond to the other extreme value which is no gas penetration and modelled by $q \to \infty$. Based on these curves we also expect that the theoretical limiting velocity may be lower than the Rayleigh wave velocity in a situation where the gas doesn't entirely fill a propagating crack.

The results presented above can only form a qualitative basis for the equation of motion of a pressurized crack in a blasting situation. If they are supplemented by an expansion law for the gaseous detonation products, an expression for the crack surface displacement, and measurements of the effective fracture surface energy γ_F as a function of the crack velocity then one may perhaps hope to use $G_I = 2\gamma_F$ as an equation of motion for crack growth, much in the same way as Bergkvist [17] has done for a central crack in an infinite sheet of PMMA.

ACKNOWLEDGEMENT

This research has been supported by the Atlas Copco and Nitro Nobel companies.

REFERENCES

1. OUCHTERLONY, F., Proc. Third Congress, ISRM IIB, 1974, 1377.
2. OUCHTERLONY, F., Int. J. Eng. Sci., in press.
3. OUCHTERLONY, F., Swedish Detonic Res. Found. Rept. 1976:13.
4. BROBERG, K. B., Arkiv för Fysik, 18, 1960, 159.
5. CRAGGS, J. W., Fracture of Solids, Wiley Interscience, New York, 1962, 51.
6. ATKINSON, C., Arkiv för Fysik, 35, 1967, 469.
7. WILLIS, J. R., Phil. Trans. Roy. Soc., A274, 1973, 435.
8. CHEREPANOV, G. P. and AFANAS'EV, E. F., Int. J. Eng. Sci., 12, 1974, 665.
9. NORWOOD, F. R., Int. J. Solids and Structures, 9, 1973, 789.
10. NORWOOD, F. R., Int. J. Eng. Sci., 14, 1976, 477.
11. BROCK, L. M., Int. J. Eng. Sci., 13, 1975, 951.
12. BROCK, L. M., Int. J. Eng. Sci., 14, 1976, 181.
13. SIH, G. C., PARIS, P. C. and ERDOGAN, F., J. Appl. Mech., 29, 1962, 306.
14. CRAGGS, J. W., Proc. Cambridge Phil. Soc., 56, 1960, 269.
15. BYRD, P. F. and FRIEDMAN, M. D., Handbook of Elliptic Integrals for Engineers and Scientists, Second Edition, Springer Berlin, 1971.
16. FREUND, L. B. and CLIFTON, R. J., J. Elasticity, 4, 1974, 293.
17. BERGKVIST, H., J. Mech. Phys. Solids, 21, 1973, 229.

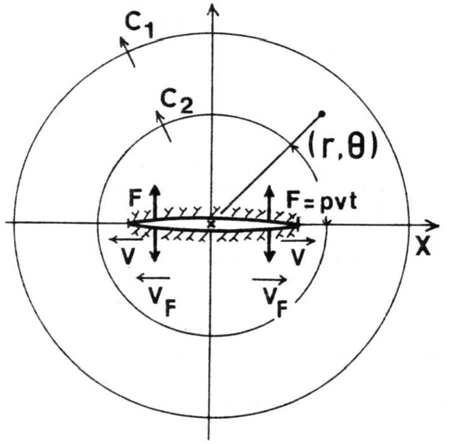

Figure 1 Crack Geometry

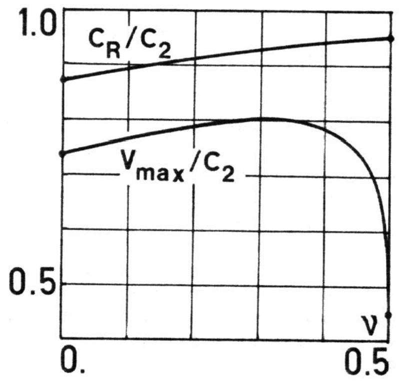

Figure 2 Limiting Crack Speeds

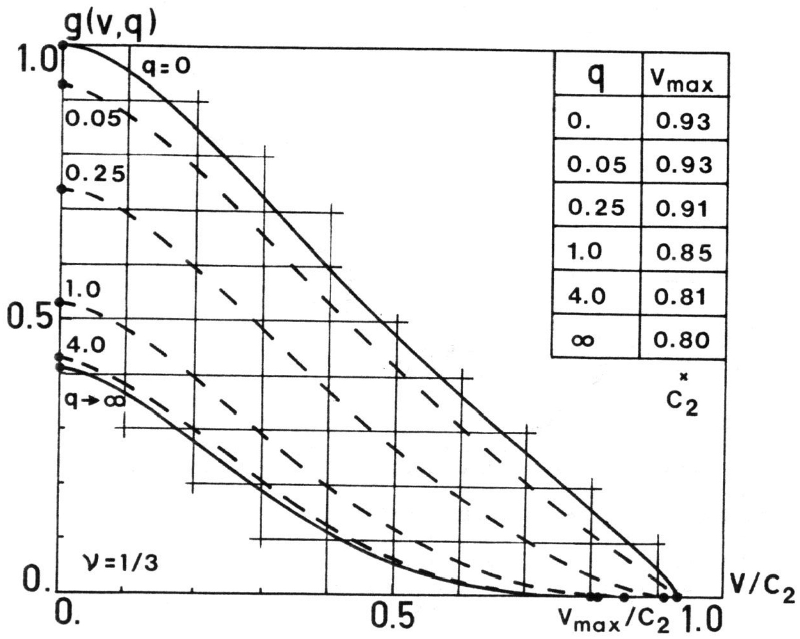

Figure 3 Normalized Energy Release Rates Versus Crack Speed